ACS Sustainable Chemistry & Engineering

Research Article

pubs.acs.org/journal/ascecg

Meso/Macroporous Silica from Miscanthus, Cereal Remnant Pellets, and Wheat Straw

Hallah Ahmad Alyosef,[†] Denise Schneider,[†] Susan Wassersleben,[†] Hans Roggendorf,[‡] Michael Weiß,[§] André Eilert,[§] Reinhard Denecke,[§] Ingo Hartmann,[∥] and Dirk Enke*[,†]

[†]Institute of Chemical Technology, University of Leipzig, Linnéstr. 3, 04103 Leipzig, Germany

[‡]Institute of Physics, Martin-Luther-University Halle-Wittenberg, Von-Dankelmann-Platz 3, 06120 Halle (Saale), Germany

[§]Wilhelm-Ostwald-Institute for Physical and Theoretical Chemistry, University of Leipzig, Linnéstr. 2, 04103 Leipzig, Germany

[∥]DBFZ Deutsches Biomasseforschungszentrum Gemeinnützige GmbH, Torgauer Str. 116, 04347 Leipzig, Germany

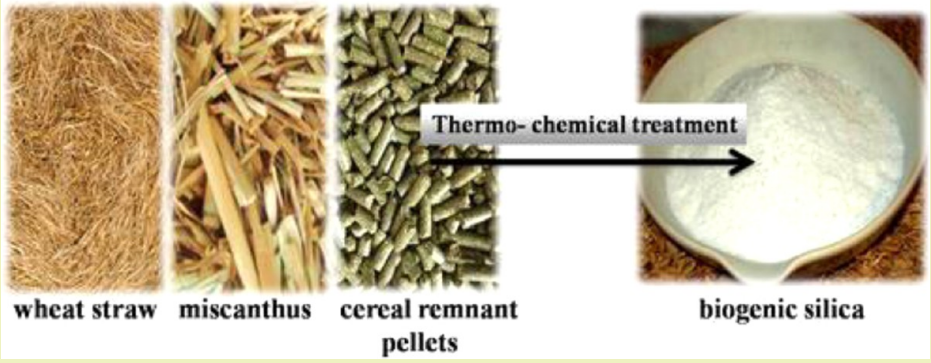

ABSTRACT: In the present study, the possibility of extracting biogenic silica from various European biomass materials was investigated. High-purity biogenic silica (>90 wt % SiO_2) was obtained from energy crops (miscanthus), agro wastes (wheat straw), and other crop residues (cereal remnant pellets). Three different morphological forms of biogenic silica materials (ash) were obtained by a thermo-chemical treatment of these biomass sources. The wet biomass materials were leached using 5 M sulfuric acid for a defined period of time. After washing and drying the biomass materials, the leached samples were subjected to a heat treatment in a furnace with three sequential temperatures and time stages to determine the minimum combustion temperature of the organic compounds in the biomass materials. The final products were characterized by X-ray diffraction, X-ray fluorescence, carbon content analysis, differential thermal analysis, low temperature nitrogen adsorption, mercury intrusion porosimetry, and scanning electron microscopy. The obtained silica materials had a microstructure composed of accessible, interconnected, and intraparticle meso- and macropores with sizes ranging from 3 to 1500 nm.

KEYWORDS: *Wheat straw, Cereal remnant pellets, miscanthus, Biogenic silica, Porosity*

INTRODUCTION

Recently, biogenic silica from rice husk ash (RHA) has been the focus of several scientific studies[1−3] due to a number of ecological, economic, and environmental considerations.[1] In addition, the presence of meso- and macropores in biogenic silica materials suggests many approaches for the preparation of value added silica (i.e., purely microporous silicalite[3]) or the synthesis of hierarchically structured materials via pseudomorphic transformation.[2,4,5] Highly purified biogenic silica of 99.8 wt % SiO_2 (rice husk ash) was recently obtained by burning rice husks that had been pretreated with citric acid.[3] The use of organic acid solutions such as citric acid during the leaching step is considered a more economical, ecological, and benign process compared to the use of inorganic acids like hydrochloric acid (HCl), nitric acid (HNO_3), or sulfuric acid (H_2SO_4).[1,6]

Burning time and temperature are equally important in removing carbon from rice husk ash, while retaining silica in an amorphous form.[1] Longer burning times at temperatures above 1073 K will cause the collapse of the cellular microstructure and the coalescence of the fine pores.[7] Consequently, the specific surface area is reduced,[8] and crystalline silica phases are formed.[9] The chemical and thermal treatment of rice husks not only provides a solution for waste product disposal but also opens up sustainable manufacturing routes to valuable silica products as renewable materials.[1−3] The availability of rice husks is continuously increasing in many developing countries, particularly in Indonesia, Bangladesh, and Vietnam.[10] However, they are currently rarely utilized in these same countries.

Received: April 6, 2015
Revised: July 15, 2015
Published: July 23, 2015

DOI: 10.1021/acssuschemeng.5b00275
ACS Sustainable Chem. Eng. 2015, 3, 2012−2021

The percentage of rice husks in paddy rice varies across different countries, influenced by various factors such as the rice species, cultivation area, soil fertility, weather, irrigation efficiency, farming practices, etc.[11,12] However, rice paddies typically contain 20 wt % rice husks on average.[11] In terms of energy production, rice husks are often used throughout the rice growing areas of the world, including the U.S., Thailand, China, etc.[13] In Europe, several lignocellulosic agricultural biomasses from energy crops (miscanthus), other crop residues (cereal remnant pellets),[14−16] and agro wastes (wheat straw)[17,18] have a huge potential as a substitute for fossil fuels.[14,15] The cultivation of miscanthus began in 1983 in Denmark; in 1987, cultivation of this crop reached Germany. Additionally, there have been some attempts to cultivate miscanthus in the United States.[19] Miscanthus is an interesting material because it includes species that are rich in carbohydrates. Several recent studies have investigated the pretreatment of miscanthus for bioethanol production,[19] hydrogen production,[20] and the extraction of lignin, xylan, glucan, and arabinan.[21] Cereal byproducts such as wheat straw and cereal remnant pellets can also be a source of value added products. For example, long natural cellulose fibers[17] and nanocellulose fibers[18] can be prepared from wheat straw. Moreover, this biomass provides approximately 14% of the world's energy needs and 35% of the energy requirements of developing countries.[22]

Crop residues (e.g., cereal straw and wheat straw) and herbaceous plants (e.g., miscanthus) consist of the following five main components: cellulose, hemicellulose, lignin, extractives, and inorganics.[23] These residues are characterized by a typical agriculture-based lignocellulosic composition. Silicon and potassium are the two major ash-forming elements of the above-mentioned biomass materials.[13] Their ratios vary depending both on the species and the geographic location (e.g., cultivation area).[23] The chemical composition of the inorganic fraction of wheat straw includes 35−67 wt % SiO_2, 14−30 wt % K_2O, 5−11 wt % CaO, and 1.2−14.7 wt % Cl as the main components. This range of values is based on different sources of wheat straw.[13] The main composition of miscanthus ash is approximately 30−40 wt % SiO_2, 20−25 wt % K_2O, 5 wt % P_2O_5, 5 wt % CaO, and 5 wt % MgO.[24,25] Therefore, the ash composition of these biomass materials makes them less favorable compared to rice husk, which has SiO_2 contents between 65 and 95 wt %.[1,3] As a result, the investigation of biogenic silica resulting from these biomass materials has been excluded in previous studies.

Several researchers have focused their attention on dilute acid pretreatment for the hydrolysis of polysaccharides (hemicellulose)[26] in miscanthus and wheat straw using different types of acid (e.g., malic, formic, and sulfuric).[19,27−30] In general, acid leaching with diluted sulfuric acid (50−300 mM) is performed at 373−473 K.[26,31] After hydrolysis, the free sugars produced can degrade to furfural (from pentoses) or to 5-hydroxymethyl furfural (HMF; from hexoses).[32−34] One major disadvantage of these byproducts is the parallel formation of ethanol.[35−37] Organic acids, such as malic acid and fumaric acid, have been alternatively used for the acid leaching of biomass. The results reported to date present an interesting starting point for the synthesis of carbon-free biogenic silica from cereals, wheat straw, and miscanthus via pretreatment with sulfuric acid. The products formed through the degradation of the free sugars can be easily burned under comparatively "mild" conditions.

This pretreatment has additional advantages. It prevents the formation of potassium silicate eutectics at 973 K in wheat straw ash[38] and lower than 873 K in miscanthus ash.[25] Furthermore, the occurrence of ternary silicates in the presence of a small amount of sodium at temperatures lower than 813 K[39] is hindered. Additionally, this chemical pretreatment can increase the purity of the resulting ash by increasing the silica content and decreasing the content of the other inorganic oxides (K_2O, CaO, MgO, P_2O_5, etc.). Without chemical pretreatment of the biomass (wheat straw), the resulting materials possess textural properties typical of charcoals after burning. Depending on the burning time and temperature, the specific surface areas vary between 2 and 350 $m^2\ g^{-1}$.[13] The fibrous texture of the silica in the ash presumably results from its deposition between cellulose fibrils in the microvoids.[40]

The present study is the first to subject three varieties of European biomass materials, wheat straw, cereal remnant pellets, and miscanthus, to a defined thermal and chemical treatment to assess the impact of acid treatment on various application-oriented parameters (purity, particle morphology, and textural properties of the resulting ashes). The materials obtained were investigated by a combination of advanced characterization techniques: particle size analysis, nitrogen adsorption, mercury intrusion porosimetry, scanning electron microscopy (SEM), X-ray diffraction (XRD), and X-ray fluorescence (XRF).

MATERIALS AND METHODS

Materials. Three different raw biomass materials of European origin were employed as biogenic silica sources. Miscanthus chips (miscanthus), wheat straw, and cereal remnant pellets were provided by the Deutsches Biomasseforschungszentrum Leipzig (DBFZ). The following materials and chemicals were also used: sulfuric acid (H_2SO_4, 96%, reagent grade; Acros Organics, Germany), citric acid ($C_6H_8O_7$, 99.5%, ACS reagent; Sigma-Aldrich, Steinheim, Germany), and cellulose ($(C_{12}H_{20}O_{10})_n$, micro crystalline; Alfa Aesar, Karlsruhe, Germany).

Methods. Biogenic silica species were extracted from three biomass materials through a thermo-chemical treatment. Only the cereal remnant pellets were completely crushed with a hammer to obtain a fraction with a small particle size before further treatment. Each biomass material was separately soaked in deionized water at a solid-to-liquid ratio of 1:10 (g mL^{-1}) for 24 h (to swell the cell walls in the particles). After soaking, the weight of miscanthus, wheat straw, and cereal remnant pellets increased by 70, 50, and 40 wt %, respectively. The wet samples were filtered and leached with hot 5 M sulfuric acid. The leaching process was carried out for a defined period of time at a solid (dry mass)-to-liquid ratio of 1:10 (g mL^{-1}), a stirring speed of 1000 rpm (mechanical stirrer, RW 20, Janke & Kunkel GmbH & Co. KG IKA-Labor Technik, Staufen, Germany) and at 353 K. A 2500 mL three-necked round-bottomed flask was used for the acid treatment. The resulting silt and remnants of the biomass materials were filtered, washed several times with deionized water, and then dried overnight at 363 K. The dried samples were sequentially burned in a ceramic crucible using a muffle furnace (type N11/H, Nabertherm, Germany) at a heating rate of 10 K min^{-1}. Sequential burning was applied using different temperatures and holding times as follows: 573 K for 60 min and 683 K for 60 min. The heating rate from 683 to 873 K was 1 K min^{-1} with a holding time of 60 min. The resulting ashes were then cooled to room temperature directly in the furnace. Some wheat straw samples were alternatively leached with citric acid (5 wt %), but the rest of the treatment was identical. This alternative was investigated to compare the behavior of both acids regarding purities and textural properties. The resulting ash samples were labeled by X A-Y-Z, where X is the name of the biomass material, A is the ash, Y is the type of acid used and Z is the leaching time in hours.

DOI: 10.1021/acssuschemeng.5b00275
ACS Sustainable Chem. Eng. 2015, 3, 2012−2021

Additionally, the miscanthus material was soaked in distilled water at 363 K for 3 h, filtered, and dried overnight at 363 K to remove the quartz impurities. The resulting samples were labeled miscanthus-washed.

Characterization. Particle size analysis of the samples was performed using a particle size analyzer CILAS 1064 (Quantachrome Instruments, Boynton Beach, FL, USA). Particle sizes were determined via static laser light scattering and calculated using Fraunhofer diffraction theory. The average particle diameters of dp_{10}, dp_{50}, and dp_{90} were determined at 10%, 50%, and 90% of the cumulative size distribution of the powder being analyzed. Each value is the average of three individual samples with their standard deviations. Elemental analysis of the samples was carried out by XRF analysis (S4 Explorer, WDXRF, Bruker, Karlsruhe, Germany). For this purpose, 1.5 g of the sample was mixed with 0.5 g of wax powder. The mixture was pressed into a 25 mm diameter disc with a load of 50 tons for 1 min in a hydraulic press (PerkinElmer, Überlingen, Germany). X-ray powder diffraction (XRD) patterns were taken on a D8 DISCOVER diffractometer (Bruker, Germany) with Cu−Kα radiation at 40 kV and 30 mA. The scanning range was from 5° to 75° 2θ in the Bragg−Brentano geometry, with a step width of 0.02° 2θ and a step time of 6 s. The mineralogical analysis of the ashes was conducted using the ICDD-PDF2 database in the DIFFRAC.SUITE EVA-XRD software (Bruker Corporation) and the Rietveld-based Seifert Auto Quant software. Fluorite (20 wt %) was added as an internal standard to determine the amorphous content. The carbon content was measured by a Vario EL microanalyzer system (Heraeus, Hanau, Germany). Thermal analyses of the biomass materials were performed using a Thermo Gravimetric/Differential Thermal Analyzer TG/DTA equipment (SDT2960 simultaneous apparatus, TA Instrument, New Castle, DE, USA) with a supplemental air flow rate of 150 mL min^{-1}. The temperature range was between 293 and 1273 K with a heating rate of 10 K min^{-1}. The textural properties of the samples were determined by nitrogen adsorption (ASAP 2010, Micromeritics, Norcross, GA, USA). Before analysis, all samples were pretreated at 363 K under vacuum for 6−8 h to obtain a constant weight. The specific surface area was evaluated using the Brunauer−Emmett−Teller (BET) model in the relative pressure range (p/p_0) of the sorption isotherm between 0.05 and 0.25.[41] The mean diameter of mesopores ($D_{mean\ 1}$) was determined from the adsorption branch of the isotherms using the Barret−Joyner−Halenda (BJH) method. The specific macropore volume and macropore size distribution were measured by mercury intrusion porosimetry (Pore Master, Quantachrome instruments, USA). A mercury surface tension of 484 erg cm^{-2} and a contact angle of 141.3° were employed. The surface morphology of the materials was investigated using a scanning electron microscope (Zeiss, Spectro Analytical Instruments GmbH, Kleve, Germany) operated at 5 keV.

RESULTS AND DISCUSSION

Thermal Behavior of the Biomass Samples. To estimate the amount of organic constituents in the initial biomass materials, the loss on ignition (LOI %) was calculated via eq 1[42] using the difference in the weight of the biomass samples before (m_0) and after (m_1) burning at 1273 K for 30 min with a heating rate of 10 K min^{-1}.

$$\text{LOI}\ (\%) = (m_0 - m_1) \times 100/m_0 \quad (1)$$

The LOI for miscanthus, wheat straw, and cereal remnant pellets was 92, 88.9, and 77.5 wt %, respectively. These pronounced LOI % values are attributed to the high content of organic matter in the biomass materials.

The thermogravimetric analysis (TG) and differential thermal analysis (DTA) of each biomass material and a commercial cellulose sample are shown in Figure 1.

The results of the thermal analysis of the studied biomass materials are quite similar to those of commercial cellulose. The

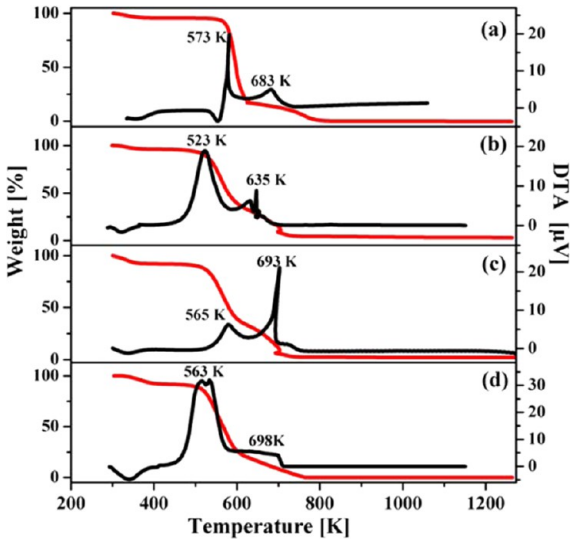

Figure 1. DTA (black curve and *y*-axis on the right-hand side) and TG (red curve and *y*-axis on the left-hand side) profiles of (a) commercial cellulose, (b) wheat straw, (c) cereal remnant pellets, and (d) miscanthus.

Table 1. Weight Loss Determined by TG Analysis of the Biomass Species (Wheat Straw, Cereal Remnant Pellets, and Miscanthus)

sample name	first weight loss [wt %]	second weight loss [wt %]	third weight loss [wt %]
miscanthus	$T_{RT\text{-}360\ K}$ = 5.9	$T_{360-604\ K}$ = 60.8	$T_{604-775\ K}$ = 25.3
cereal remnant pellets	$T_{RT\text{-}327\ K}$ = 8.8	$T_{327-585\ K}$ = 52.3	$T_{585-753\ K}$ = 28.0
wheat straw	$T_{RT\text{-}315\ K}$ = 4.4	$T_{315-569\ K}$ = 55.2	$T_{569-707\ K}$ = 27.9

biomass species exhibit an endothermic heat effect, with the maximum peak temperature at 315 K, 327 K, and 360 K for wheat straw, cereal remnant pellets, and miscanthus, respectively. This is characteristic for the removal of physisorbed water.

This process is accompanied by a consecutive weight loss of 4.4, 8.8, and 5.9 wt % (Table 1).

The wheat straw and cereal remnant pellets display two exothermic heat effects. A low temperature peak (523 K for wheat straw with a weight loss of 55.2 wt % and 565 K for cereal remnant pellets with a weight loss of 52.3 wt %) is generally caused by the decomposition of hemicellulose and lignin compounds accompanied by cellulose.[8] The main peak at a higher temperature is attributed to cellulose degradation[3,6] (635 K for wheat straw with a weight loss of 27.9 wt % and 693 K for cereal remnant pellets with a weight loss of 28 wt %). Miscanthus exhibits a broad exothermic heat effect with a maximum peak temperature of 563 K. A pronounced weight reduction of 64.8 wt % is observed in this temperature range. The second exothermic heat effect appears as a broad shoulder with a weight loss of 25.3 wt % between 604 and 775 K. Furthermore, the two exothermic heat effects in all samples studied indicate that the major weight loss corresponds to the cellulose, hemicellulose, and lignin components, which are the organic components in the biomass.[8,23] The presence of high concentrations of potassium and other basic species in biomass material (wheat straw and rice straw) has a considerable influence on the thermal decomposition process and particularly on the thermal degradation of cellulose.[13,43]

DOI: 10.1021/acssuschemeng.5b00275
ACS Sustainable Chem. Eng. 2015, 3, 2012−2021

Table 2. Chemical Analysis of the Inorganic Fraction (= 100%) of the Wheat Straw and Wheat Straw Ash Obtained by the Combustion of the Samples Pre-treated with Sulfuric Acid or Citric Acid

constituent	wheat straw [wt %]	wheat straw A-H_2SO_4-3 [wt %]	wheat straw A-H_2SO_4-6 [wt %]	wheat straw A-H_2SO_4-12 [wt %]	wheat straw A-H_2SO_4-24 [wt %]	wheat straw A-$C_6H_8O_7$-24 [wt %]
SiO_2	40.5	59.0	70.6	83.4	92.8	65.7
Al_2O_3	0.2	0.5	0.2	0.1	0.0	0.1
Fe_2O_3	0.8	0.2	0.1	0.1	0.0	0.1
CaO	15.8	7.2	5.2	3.3	2.8	9.8
MgO	1.3	0.8	0.5	0.2	0.1	1.1
K_2O	34.3	13.0	9.3	5.8	0.8	15.8
P_2O_5	1.3	0.8	0.5	0.2	0.0	1.0
Cl	1.0	0.2	0.2	0.1	0.1	0.6
SO_3	6.7	17.0	12.5	5.5	0.7	4.3
others[a]	0.7	1.3	0.9	1.3	2.7	1.5

[a]Other inorganic oxides.

Table 3. Chemical Analysis of the Inorganic Fraction (= 100%) of the Cereal Remnant Pellets, Miscanthus and Their Ashes Resulting from Burning of the Samples Pre-treated with Sulfuric Acid

constituent	cereal remnant pellets [wt %]	miscanthus [wt %]	cereal remnant pellets A-H_2SO_4-24 [wt %]	miscanthus A-H_2SO_4-24 [wt %]
SiO_2	28.0	47.0	91.3	95.0
Al_2O_3	1.8	5.3	1.4	1.8
Fe_2O_3	4.6	6.3	0.1	0.3
CaO	24.5	11.9	2.7	0.5
MgO	1.8	1.0	0.5	0.0
K_2O	23.5	18.9	1.1	1.2
Cl	1.5	0.0	0.7	0.0
P_2O_5	7.3	0.0	0.2	0.0
SO_3	5.8	5.3	0.8	0.9
others[a]	1.2	4.3	1.2	0.3

[a]Other inorganic oxides.

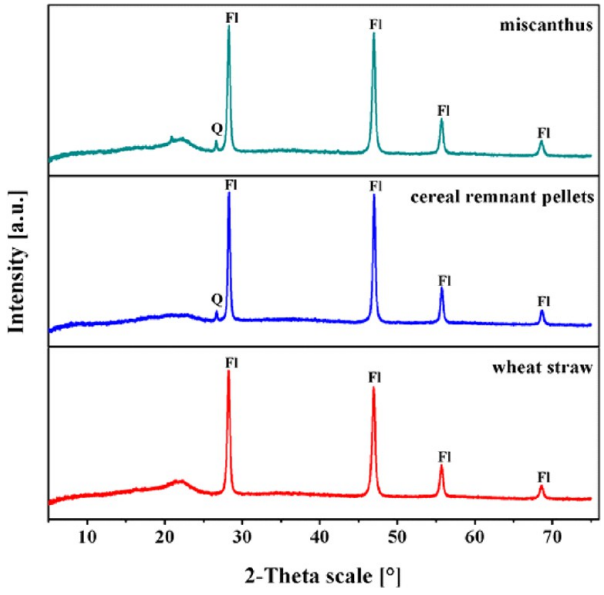

Figure 2. XRD patterns of the initial biomass samples. Q, quartz; Fl, the internal standard fluorite.

However, potassium is considered one of the major inorganic components in the biomass materials studied (Tables 2 and 3). Compared to commercial cellulose, the formation of potassium species[44−46] during the thermal decomposition of biomass materials shifts the maximum peak temperature of the first exothermic heat effect to lower values (Figure 1). Additionally, it is not easy to design a unique procedure for the combustion

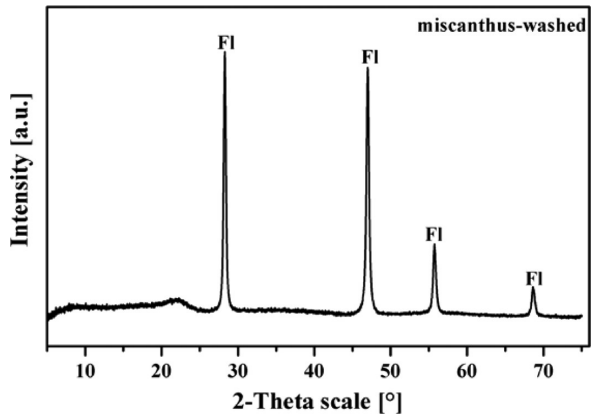

Figure 3. XRD pattern of the miscanthus-washed sample. Fl, the internal standard fluorite.

Table 4. Quantitative XRD Phase Analysis of Initial Biomass Samples and the Miscanthus-Washed Sample

phase	wheat straw [wt %]	cereal remnant pellets [wt %]	miscanthus [wt %]	miscanthus-washed [wt %]
quartz	0.0	0.8	1.9	0.0
amorphous phase	100	99.2	98.1	100

Table 5. Quantitative XRD Phase Analysis of Ash Samples Resulting from Burning of Biomass Pre-treated with Sulfuric Acid for 24 h

phase	wheat straw A-H_2SO_4-24 [wt %]	cereal remnant pellets A-H_2SO_4-24 [wt %]	miscanthus A-H_2SO_4-24 [wt %]
quartz	0.6	11.6	8.9
anhydrite[a]		0.8	4.9
arcanite[b]	22.8		
feldspar K (orthoclase)[c]	6.9	3.3	1.9
amorphous phase	69.7	84.3	84.2

[a]$CaSO_4$-anhydrite. [b]K_2SO_4-arcanite. [c]KSi_3AlO_8-feldspar K (orthoclase).

DOI: 10.1021/acssuschemeng.5b00275
ACS Sustainable Chem. Eng. 2015, 3, 2012−2021

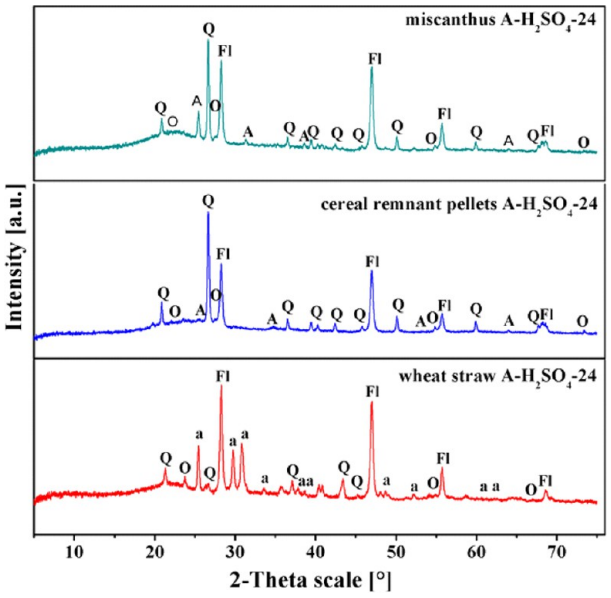

Figure 4. XRD patterns of ash samples resulting from the burning of biomass pretreated with sulfuric acid for 24 h. Q, quartz; O, feldspar K (orthoclase); A, anhydrite; a, arcanite; Fl, the internal standard fluorite.

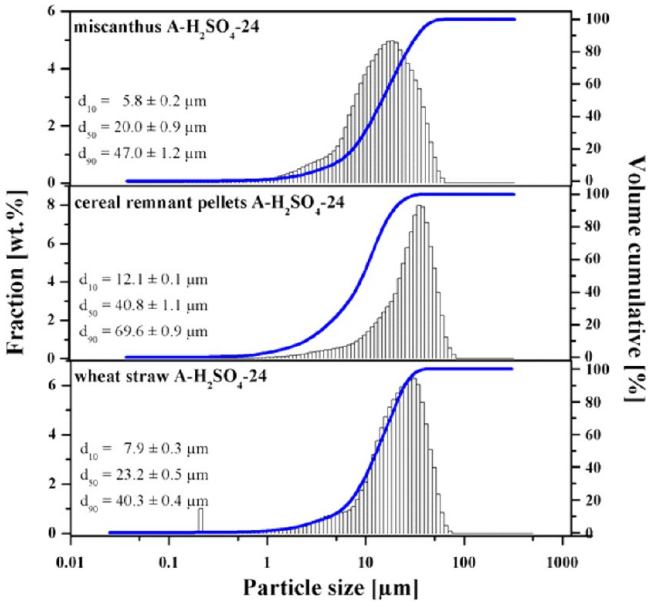

Figure 5. Particle size distribution (column chart and *y*-axis on the left-hand side) and cumulative volume of pores (line diagram and *y*-axis on the right-hand side) of ashes resulting from the burning of biomass leached with sulfuric acid for 24 h.

of different biomass materials due to the formation of nonhomogenous phases (silt and remaining biomass materials) in different ratios in the individual samples during the acid leaching step.Thus, there is no complete hydrolysis of the organic compounds (particularly cellulose) during the acid treatment, especially when using citric acid.

However, to design the initial practical parameters for the combustion of all acid-leached biomass materials, the burning temperatures are selected based on the application of the maximum peak temperatures of the exothermic heat effects of commercial cellulose. For the first burning step at 573 K for 60 min, the maximum temperature of the thermal degradation of

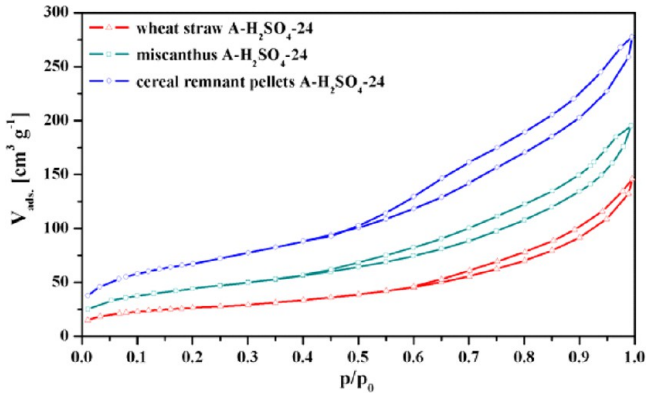

Figure 6. Nitrogen adsorption−desorption isotherms of ash samples resulting from the burning of biomass leached with sulfuric acid for 24 h.

Table 6. Textural Properties of the Ash Resulting from the Burning of Samples Pretreated with Sulfuric Acid for 24 h

sample specification	$A_{B.E.T.}$ [m² g⁻¹] [a]	$D_{mean\ 1}$ [nm] [a]	$D_{mean\ 2}$ [nm] [b]	$D_{mean\ 3}$ [µm] [c]	$V_{P,cum}$ [cm³ g⁻¹] [d]
wheat straw A-H_2SO_4-24	95	7.5	1200	29	4.8
cereal remnant pellets A-H_2SO_4-24	245	7.6	1400	36	3.1
miscanthus A-H_2SO_4-24	160	7.3	1100	25	5.5

[a]Nitrogen adsorption. [b]Mercury intrusion porosimetry, mean pore diameter, pressure part (10−400 MPa). [c]Mercury intrusion porosimetry mean pore diameter, pressure part (0.02−10 MPa). [d]Mercury intrusion porosimetry, whole pressure range.

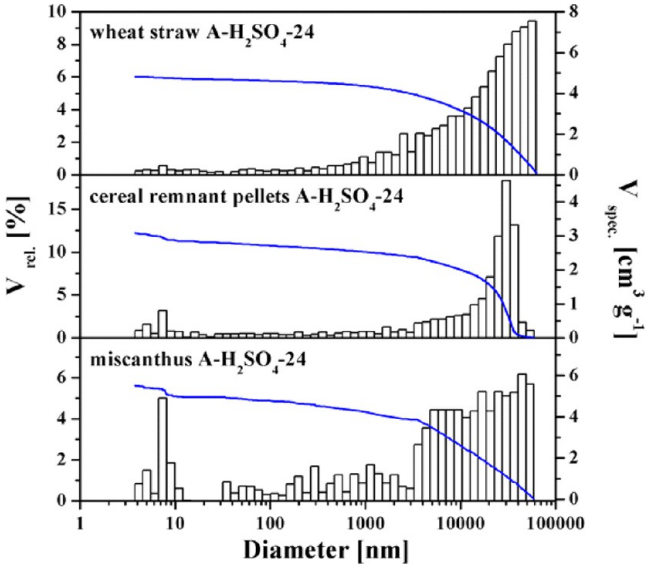

Figure 7. Differential (column chart and *y*-axis on the left-hand side) and cumulative (line diagram and *y*-axis on the right-hand side) pore volume distributions of ash samples obtained by the burning of biomass leached with sulfuric acid for 24 h.

cellulose is applied. In this case, hemicelluloses and lignin undergo thermal degradation. After 1 h, the end of the first process is indicated by the absence of any smoke released from the resulting black ash. The selected burning temperature of 683 K with a holding time of 60 min for the second stage corresponds to the maximum peak temperature of the second

DOI: 10.1021/acssuschemeng.5b00275
ACS Sustainable Chem. Eng. 2015, 3, 2012−2021

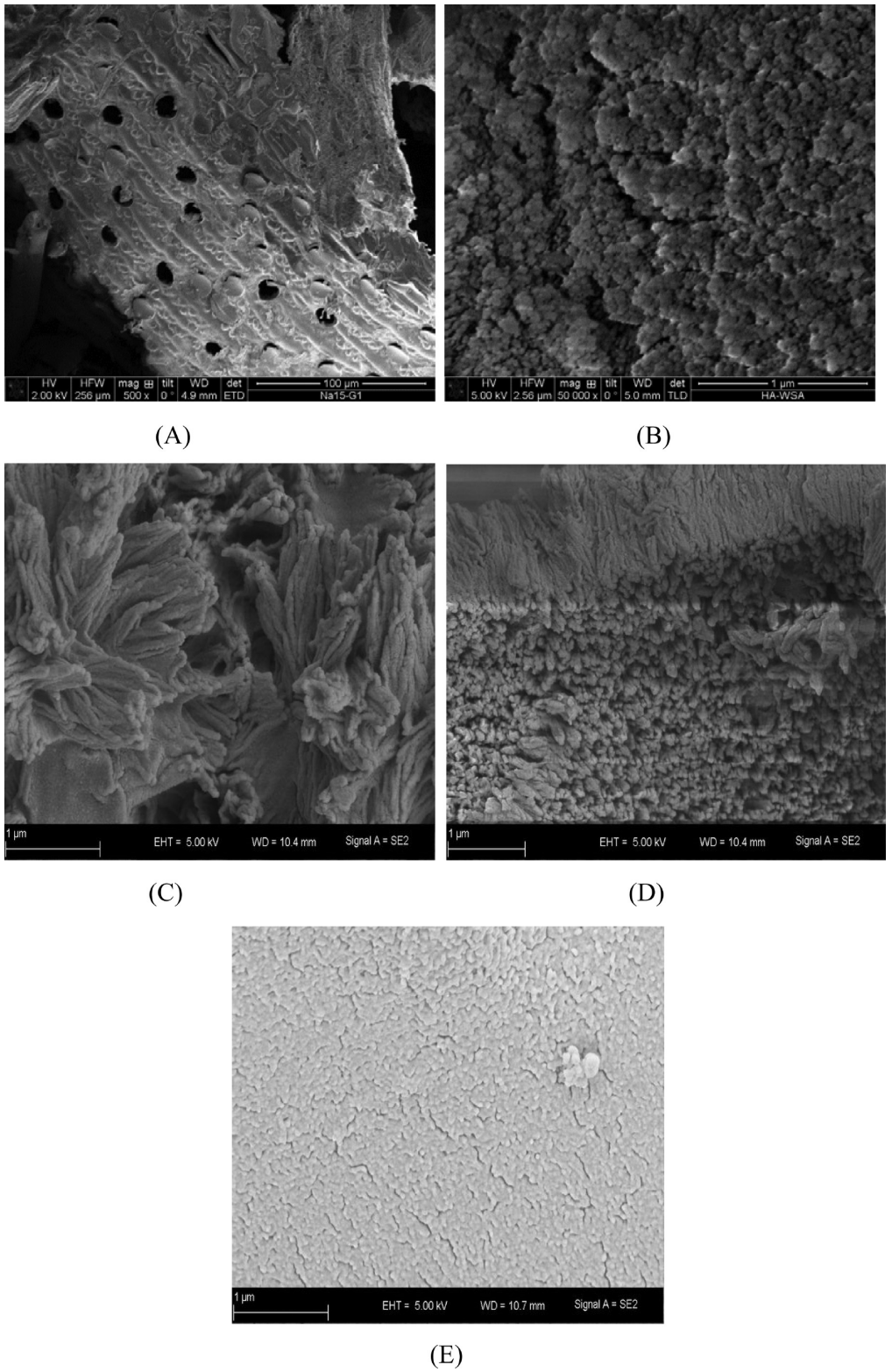

Figure 8. SEM images of wheat straw A-H_2SO_4-24 (A in outer epidermis; B in inner epidermis), cereal remnant pellets A-H_2SO_4-24 (C in outer epidermis; D in inner epidermis), and miscanthus A-H_2SO_4-24 (E in outer epidermis).

exothermic heat effect of commercial cellulose. This step is necessary to prevent carbonization (the conversion of an organic substance into carbon) of any organics in the resulting ash.[1,6] During the temperature increase from 683 to 873 K, a slow heating rate of 1 K min^{-1} is essential to complete the combustion of the carbon in the ash, which is released as CO_2, to obtain white ash. The burning temperature of 873 K, the last step in the optimized burning procedure, represents the high temperature range in the second exothermic heat effect of commercial cellulose.

Impact of the Pretreatment Process on the Chemical Composition of the Inorganic Fraction of Wheat Straw

DOI: 10.1021/acssuschemeng.5b00275
ACS Sustainable Chem. Eng. 2015, 3, 2012−2021

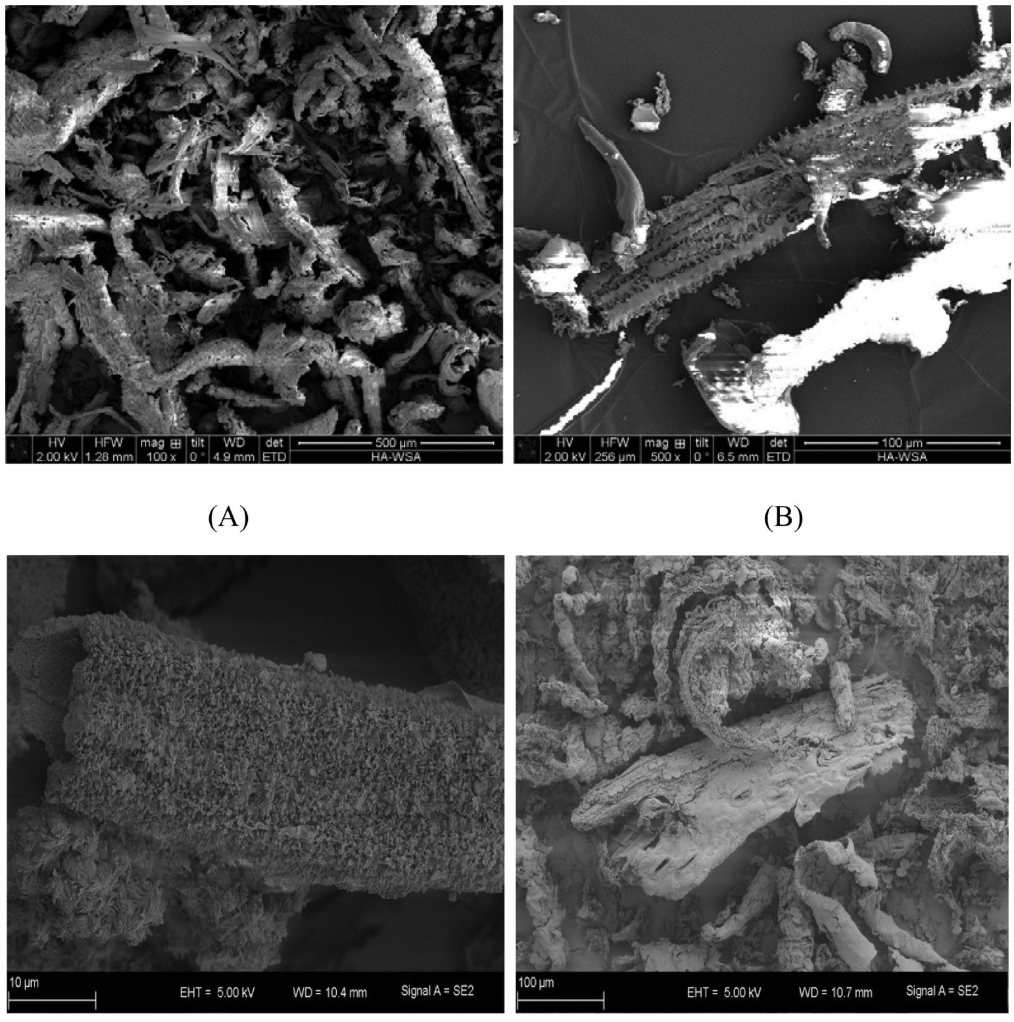

Figure 9. SEM images of the skeleton body of wheat straw A-H_2SO_4-24 (A,B), miscanthus A-H_2SO_4-24 (C), and cereal remnant pellets A-H_2SO_4-24 (D) samples.

Ash. The inorganic components of the wheat straw and wheat straw ash samples are shown in Table 2. The treatment time for wheat straw with sulfuric acid varied between 3 and 24 h, and two types of acids were applied for the leaching process, sulfuric acid and citric acid. The wheat straw samples leached in sulfuric acid were burned at 873 K to obtain ash samples that are named wheat straw A-H_2SO_4-3, wheat straw A-H_2SO_4-6, wheat straw A-H_2SO_4-12, and wheat straw A-H_2SO_4-24.

Potassium, calcium, and sulfur compounds (K_2O, CaO, and SO_3) are the major impurities present in the ash samples. Significant effects on the composition of the resulting ashes are due to the increase in the leaching time. The maximum silica content was obtained after 24 h of leaching with 92.8 wt % for wheat straw A-H_2SO_4-24. The relative reductions of K_2O, CaO, and SO_3 are 98%, 82%, and 90%, respectively, while Al_2O_3, MgO, Cl, and P_2O_5 are almost completely removed.

The ash obtained from wheat straw leached with citric acid (wheat straw A-$C_6H_8O_7$-24) still contains a high amount of inorganic impurities (34.3 wt %). The incomplete potassium extraction is caused by the hydrolysis of organic compounds (cellulose and hemicellulose) during the formation of monosaccharides.[32] The monosaccharides are assumed to hinder the access of the leaching agent to the inorganic impurities. As a result, the volatilization of potassium is hindered by its fixation to the organic matrix at temperatures below 673 K.[47] This process could have also affected the residues of other inorganic impurities in the wheat straw A-$C_6H_8O_7$-24 sample. Nevertheless, the chemical composition of the inorganic fraction was altered by citric acid leaching when comparing wheat straw with the resulting ash (i.e., wheat straw A-$C_6H_8O_7$-24) (Table 2). The silica content increases from 40.5 to 65.7 wt %. In addition, a marked reduction of the total content of metal and nonmetal oxide impurities is observed. Furthermore, due to the different behavior of citric acid and sulfuric acid during acid treatment of the wheat straw samples, variations in the carbon content in the resulting ashes are observed. The carbon content (not included in Table 2, but determined separately) decreases from 44.4 wt % in the wheat straw sample to a trace level in wheat straw A-H_2SO_4-24, whereas approximately 5.8 wt % of carbon is observed in wheat straw A-$C_6H_8O_7$-24.

Comparative Study of the Different Biomass Materials. *Elemental, Phase, and Particle Size Analysis of the Biomass Samples.* Table 3 lists the results of the chemical

DOI: 10.1021/acssuschemeng.5b00275
ACS Sustainable Chem. Eng. 2015, 3, 2012−2021

analysis of the inorganic components of the cereal remnant pellets, miscanthus, and their ashes obtained by burning of the samples pretreated with sulfuric acid.

The silica content is relatively low in all of the biomass materials (Tables 2 and 3). In addition, the carbon content (not included in Tables 2 and 3 but determined separately) is 44.5, 41.5, and 44.4 wt % for miscanthus, cereal remnant pellets, and wheat straw samples, respectively.

The sulfuric acid treatment was applied to remove impurities and improve the microstructural properties of the ashes. These results demonstrate the marked effect of the sulfuric acid leaching on removing or decreasing the contents of most accompanying oxides relative to SiO_2 (Tables 2 and 3). The ash samples contain less than 10 wt % of nonsilica impurities. The main component of the ash samples in each case was SiO_2 with additional lower contents of the oxides of K, Ca, and other impurities. The silica content amounts to 91.3, 92.8, and 95.0 wt % for the cereal remnant pellets, wheat straw, and miscanthus samples (A-H_2SO_4-24), respectively. In addition, the content of potassium oxide consecutively decreases to 1.1, 0.8, and 1.2 wt %. The white color of the resulting ashes is an indication of the completeness of combustion and the low level of remaining inorganic impurities.

The XRD patterns and quantitative XRD phase analysis of the initial biomass materials and the miscanthus-washed sample are shown in Figures 2 and 3 and Table 4.

A minor phase of quartz represented by a peak with a lower intensity at 2θ of 26.6° is observed in the cereal remnant pellets and miscanthus samples. However, the content of quartz is less than 2 wt %, whereas a pure amorphous phase was found in the wheat straw and miscanthus-washed samples. The broad peak in the range of 2θ = 18−28° was essentially due to the amorphous silica in all of the analyzed samples.

Table 5 and Figure 4 present the quantitative XRD phase analysis and XRD patterns of the ash samples resulting from burning samples pretreated with sulfuric acid for 24 h.

In addition to the amorphous phase, quartz is the main crystalline phase in cereal remnant pellets A-H_2SO_4-24 and miscanthus A-H_2SO_4-24 samples. Two minor crystalline phases are anhydrite and feldspar K (orthoclase), represented by a multitude of peaks with lower intensities. However, wheat straw A-H_2SO_4-24 contains arcanite (K_2SO_4) as the main crystalline constituent, whereas only traces of anhydrite ($CaSO_4$) and quartz are observed. Approximately equal amounts of 80 wt % amorphous silica are present in the cereal remnant pellets A-H_2SO_4-24 and miscanthus A-H_2SO_4-24 samples. The wheat straw A-H_2SO_4-24 sample contains approximately 70 wt % of amorphous silica. In addition, the quartz content increases in all ashes derived from biomasses leached in sulfuric acid due to combustion. Obviously, a part of the amorphous silica has been transformed into quartz during this thermal treatment. A very low quartz content <1 wt % is observed in wheat straw A-H_2SO_4-24.

Feldspar K (KSi_3AlO_8, orthoclase) is clearly detectable in all of the resulting ashes, whereas arcanite is formed only in wheat straw A-H_2SO_4-24. The formation of the last two phases could be due to a thermodynamic effect ("back formation" of feldspar or arcanite through reduction of part of the amorphous silica).[48] The remaining low concentrations of Al_2O_3, CaO, and K_2O in the ashes (Tables 2 and 3) can be assigned to phases such as feldspar K, arcanite, and anhydrite, as confirmed by XRD.

Figure 5 shows the particle size analysis of the ash samples resulting from the burning of biomass leached with sulfuric acid for 24 h.

The ashes have a unimodal particle size distribution.[49] The highest mean particle diameter dp_{50} of 41.1 μm corresponds to cereal remnant pellets A-H_2SO_4-24, followed by wheat straw A-H_2SO_4-24 (dp_{50} = 23.8 μm) and miscanthus A-H_2SO_4-24 (dp_{50} = 22.3 μm). The particle size distribution of cereal remnant pellets A-H_2SO_4-24 shifts to the highest values compared to that of the other two samples. However, the presence of mineral impurities (e.g., feldspar and quartz) in the resulting ashes can increase the specific gravity and particle size.[48]

Properties of the Pore Structure. Figure 6 shows the nitrogen sorption isotherms of the ashes resulting from the burning of biomass leached with sulfuric acid for 24 h.

According to the IUPAC nomenclature, the isotherms exhibit the common characteristics of a type IV isotherm of Brunauer's classification with a closed hysteresis loop.[50] The nitrogen adsorption isotherms are characterized by a small knee at p/p_0 = 0.05, which is followed by a continuous increase in the nitrogen uptake to high p/p_0 values. No saturation at relative pressure ratios close to unity is observed because the samples contain meso- and macropores with very broad size distributions.[48,51] Furthermore, the isotherms are characterized by a lower closure point of the hysteresis loops at approximately p/p_0 = 0.60, 0.50, and 0.45 for wheat straw A-H_2SO_4-24, cereal remnant pellets A-H_2SO_4-24, and miscanthus A-H_2SO_4-24 samples, respectively. The presence of the hysteresis loop in the isotherms studied is due to the existence of larger mesopores in the ashes.[48,51]

Table 6 summarizes the textural properties of the ashes produced by the thermo-chemical treatment of wheat straw, cereal remnant pellets, and miscanthus.

Furthermore, the specific surface area ($A_{B.E.T}$) of the ashes produced from the different biomass materials varies even when applying the same procedure during the thermo-chemical treatment (Table 5). Thus, the highest values of $A_{B.E.T}$ corresponds to cereal remnant pellets A-H_2SO_4-24 at 245 m^2 g^{-1}, followed by miscanthus A-H_2SO_4-24 at 160 m^2 g^{-1}, and wheat straw A-H_2SO_4-24 at 95 m^2 g^{-1}.

The macropore size range of the samples was investigated by mercury intrusion porosimetry. The corresponding pore size distributions are depicted in Figure 7.

The results shown in Figure 7 indicate that all of the ash samples are characterized by a very broad pore-size distribution of the intraparticle meso- and macropores and interstitial macropores. Approximately 27%, 22%, and 12.5% of the total cumulative pore volume ($V_{P,cum}$, see Table 6) of wheat straw A-H_2SO_4-24, cereal remnant pellets A-H_2SO_4-24, and miscanthus A-H_2SO_4-24, respectively, are formed by the intraparticle meso- and macropores. The total cumulative pore volume ($V_{P,cum}$) contains additional contributions from interstitial macropores. The total porosity of miscanthus A-H_2SO_4-24 is higher than that of wheat straw A -H_2SO_4-24 or cereal remnant pellets A-H_2SO_4-24 (Table 6).

The results of the mercury intrusion porosimetry and N_2 adsorption experiments are confirmed by the SEM images, which are shown in Figures 8A−E. The pore size of the ashes covers a wide range of intraparticle meso- and macropores between 3 nm and 1.5 μm. This property has a marked effect on the generation of a high specific surface area.

The intraparticle meso- and macropores are located in the outer and inner epidermis of the skeleton body of the ashes.

DOI: 10.1021/acssuschemeng.5b00275
ACS Sustainable Chem. Eng. 2015, 3, 2012−2021

Figure 8A–E clearly shows that the resulting ashes from the biomass materials possess several pore shapes and sizes in the outer and inner epidermis of their skeleton body. The biological morphology is preserved during combustion, but the materials are transformed into inorganic phases. This "pseudomorphosis" governs the structure and pore morphology. Some pores have round shapes with sizes between 0.1–1.5 μm (Figure 8A). Other pores display irregular slit-shapes with various sizes ranging between 50–1500 nm (Figure 8B–E) that resemble the voids between lamellae or fibers.

Scanning electron micrographs of the skeleton body of wheat straw A-H_2SO_4-24, cereal remnant pellets A-H_2SO_4-24, and miscanthus A-H_2SO_4-24 are shown in Figure 9A–D. Evidently, the morphology of wheat straw A-H_2SO_4-24 exhibits a backbone structure with dimensions of between 100 and 500 μm (Figure 9A–B). The cylindrical skeleton bodies of cereal remnant pellets A-H_2SO_4-24 possess a size of approximately 40 μm (Figure 9C). The SEM images of miscanthus A-H_2SO_4-24 indicate that their morphological structures are formed in the shape of a backbone or stem with dimensions ranging between 100 and 370 μm (Figure 9D).

CONCLUSIONS

This study provides a strategy for the generation of primarily amorphous porous biogenic silica from European biomass materials, such as wheat straw, cereal remnant pellets, and miscanthus. There are several barriers for the wider use of biogenic silica from rice husks in Europe, such as the limited cultivation of rice in Europe and the cost of rice husk transportation between Asia and Europe. Therefore, this article is the first to describe the criteria for the sustainable generation of biogenic silica from European biomass feedstocks.

The transformation of wheat straw into wheat straw ash was investigated in detail. For wheat straw ash leached with sulfuric acid, a clear dependence on leaching time was observed. A comparison of the properties of the wheat straw ash obtained after leaching with sulfuric acid or citric acid indicated several chemical benefits of sulfuric acid leaching: (i) a higher silica content (>90 wt %) and (ii) complete combustion of carbon.

Comparing the ashes obtained after the burning of the three different biomass materials leached with sulfuric acid for 24 h, the following conclusions can be drawn: (1) The amount of silica in all of the samples increases (>90 wt %) with the absence of any trace of carbon. However, the high content of silica is due to the presence of quartz, feldspar K (orthoclase), and amorphous phases in the end products. (2) The textural parameters of the ashes are highly dependent on the quality of the initial biomass materials and on the properties, especially the purities, of the ashes. Furthermore, the highest specific surface area (245 m^2 g^{-1}) and the highest content of amorphous biogenic silica (85 wt %) were obtained for cereal remnant pellet ash.

However, the formation of crystalline phases in most of the ashes represents a major disadvantage for their further applications as "pure" amorphous biogenic silica. Therefore, the conditions of the acid leaching treatment of the biomass materials should be studied in further detail. Additionally, the burning process should be modified to prevent the formation of quartz.

After these improvements have been made, production of value added silica products, which can already be achieved from the amorphous silica in rice husk ash, should also be possible from miscanthus, wheat straw, or cereal remnant pellets. Additional applications might result from an ordered mesopore structure obtained by pseudomorphic transformation[2,4,5] with preservation of the original macropores and the macroscopic morphology of the initial biogenic silica sources.

AUTHOR INFORMATION

Corresponding Author

*Tel: +49-34197-36302. Fax: +49-34197-36349. E-mail: dirk.enke@uni-leipzig.de.

Notes

The authors declare no competing financial interest.

ACKNOWLEDGMENTS

We express our deepest gratitude to the BMWi (Federal Ministry for Economic Affairs and Energy, Germany) and AIF (German Federation of Industrial Research Associations) for financial assistance under grant number KF2579608.

REFERENCES

(1) Ahmad Alyosef, H.; Eilert, A.; Welscher, J.; Ibrahim, S. S.; Denecke, R.; Schwieger, W.; Enke, D. Characterization of biogenic silica generated by thermo chemical treatment of rice husk. *Part. Sci. Technol.* **2013**, *31*, 524–532.

(2) Ahmad Alyosef, H.; Uhlig, H.; Münster, T.; Kloess, G.; Einicke, W.-D.; Gläser, R.; Enke, D. Biogenic silica from rice husk ash - Sustainable sources for the synthesis of value added silica. *Chem. Eng. Trans.* **2014**, *37*, 667–672.

(3) Ahmad Alyosef, H. Rice Husk Ash (RHA) as a Renewable Source for Value Added Silica Products: The Way to Standardized Educts, Comprehensive Characterization, Modification and Phase Transformation. Ph.D. Thesis, Universität Leipzig, Germany, 2014.

(4) Enke, D.; Inayat, A.; Reinhardt, B.; Uhlig, H.; Einicke, W.-D. Silica monoliths with hierarchical porosity obtained from porous glasses. *Chem. Soc. Rev.* **2013**, *42*, 3753–3764.

(5) Uhlig, H.; Gimpel, M.-L.; Inayat, A.; Gläser, R.; Schwieger, W.; Einicke, W.-D.; Enke, D. Transformation of porous glasses into MCM-41 containing geometric bodies. *Microporous Mesoporous Mater.* **2013**, *182*, 136–146.

(6) Umeda, J.; Kondoh, K. High Purity Amorphous silica originated in rice husks via carboxylic acid leaching process. *J. Mater. Sci.* **2008**, *43*, 7084–7090.

(7) Patel, M.; Karera, A.; Prasanna, P. Effect of thermal and chemical treatments on carbon and silica contents in rice husk. *J. Mater. Sci.* **1987**, *22*, 2457–2464.

(8) Hunt, L. P.; Dismukes, J. P.; Amick, J. A. Rice hull as a raw material for producing silicon. *J. Electrochem. Soc.* **1984**, *131*, 1683–1686.

(9) Amick, J. A. Purification of rice hulls as a source of solar grade silicon for solar cells. *J. Electrochem. Soc.* **1982**, *129*, 864–866.

(10) http://faostat.fao.org/site/339/default.aspx.

(11) Beagle, E. C. *Rice Husk Conversion to Energy. Food Agricultural Services Bulletin*; Food and Agriculture Organization of the United Nations: Rome, Italy, 1978.

(12) Bhattacharya, S. C.; Arul Joe, M.; Kandhekar, Z.; Abdul Salam, P.; Shrestha, R. M. Greenhouse-gas emission mitigation from the use of agricultural residues: the case of rice husk. *Energy* **1999**, *24*, 43–59.

(13) Dodson, J. R. Wheat Straw Ash and Its Use as a Silica Source. Ph.D. Thesis, University of York Chemistry: United Kingdom, 2011.

(14) Dornburg, V.; Teemer, G.; Faaij, A. Economic and greenhouse gas emission analysis of bioenergy production using multi-product crops - case studies for the Netherlands and Poland. *Biomass Bioenergy* **2005**, *28*, 454–474.

(15) Dornburg, V.; Teemer, G.; Faaij, A. Estimating GHG emission mitigation supply curves of large-scale biomass use on a country level. *Biomass Bioenergy* **2007**, *31*, 46–65.

(16) Kauter, D.; Lewandowski, I.; Claupein, W. Quantity and quality of harvestable biomass from populus short rotation coppice for solid

DOI: 10.1021/acssuschemeng.5b00275
ACS Sustainable Chem. Eng. 2015, 3, 2012–2021

fuel use -a review of the physiological basis and management influences. *Biomass Bioenergy* **2003**, *24*, 411−427.
(17) Reddy, N.; Yang, Y. Preparation and characterization of long natural cellulose fibers from wheat straw. *J. Agric. Food Chem.* **2007**, *55*, 8570−8575.
(18) Montaño-Leyva, B.; Rodriguez-Felix, F.; Torres-Chávez, P.; Ramirez-Wong, B.; López-Cervantes, J.; Sanchez-Machado, D. Preparation and characterization of durum wheat (Triticum durum) straw cellulose nano fibers by electrospinning. *J. Agric. Food Chem.* **2011**, *59* (3), 870−875.
(19) Sørensen, A.; Teller, P. J.; Hilstrom, T.; Ahring, B. K. Hydrolysis of miscanthus for bioethanol production using dilute acid presoaking combined with wet explosion petreatment and enzymatic treatment. *Bioresour. Technol.* **2008**, *99* (14), 6602−6607.
(20) de Vrije, T.; de Haas, G. G.; Tan, G. B.; Keijsers, E. R. P.; Claassen, P. A. M. Pretreatment of miscanthus for hydrogen production by thermotogaelfii. *Int. J. Hydrogen Energy* **2002**, *27*, 1381−1390.
(21) Bauer, S.; Sorek, H.; Mitchell, V. D.; Ibáñez, A. B.; Wemmer, D. E. Characterization of miscanthus giganteus lignin isolated by ethanol organosolv process under reflux condition. *J. Agric. Food Chem.* **2012**, *60*, 8203−8212.
(22) Demirbas, A. Combustion characteristics of different biomass fuels. *Prog. Energy Combust. Sci.* **2004**, *30*, 219−230.
(23) Barneto, A.; Carmona, J.; Alfonso, J. E.; Alcaide, L. Use of autocatalytic kinetics to obtain composition of lignocellulosic materials. *Bioresour. Technol.* **2009**, *100*, 3963−3973.
(24) Moilanen, A.; Nieminen, M.; Sipila, K.; Kurkela, E. Ash Behavior in Thermal Fuidized Bed Conversion Processes of Woody and Herbaceous Biomass. In *Biomass for Energy and the Environment*, Proceedings of the 9th European Bioenergy Conference, Jun 1996; Pergamon-Elsevier Publishers: Copenhagen, Denmark, 1996; pp 1227−1232.
(25) Hallgren, A. L.; Oskarsson, J. Minimization of Sintering Tendencies in Fluidized-Bed Gasification of Energy Crop Fuels. In *Biomass for Energy and Industry*; Proceedings of the 10th European Biomass Conference, Würzburg, Germany, Jun 1998; C.A.R.M.E.N. Publishers: Rimpar, Germany, 1998; pp 1700−1703.
(26) Yang, B.; Wyman, C. E. Pretreatment: the key to unlocking low-cost cellulosic ethanol. *Biofuels, Bioprod. Biorefin.* **2008**, *2*, 26−40.
(27) Allen, S. G.; Schulman, D.; Lichwa, J.; Antal, M. J. A comparison between hot liquid water and steam fractionation of corn fiber. *Ind. Eng. Chem. Res.* **2001**, *40*, 2934−2941.
(28) Duarte, L. C.; Silva-Fernandes, T.; Carvalheiro, F.; Girio, F. M. Dilute acid hydrolysis of wheat straw oligosaccharides. *Appl. Biochem. Biotechnol.* **2009**, *153*, 116−126.
(29) Kootstra, A. M. J.; Beeftink, H. H.; Scott, E. L.; Sanders, J. P. M. comparison of dilute mineral and organic acid pretreatment for enzymatic hydrolysis of wheat straw. *Biochem. Eng. J.* **2009**, *46*, 126−131.
(30) Kootstra, A. M. J.; Beeftink, H. H.; Scott, E. L.; Sanders, J. P. M. Optimization of the Dilute Maleic Acid Pretreatment of Wheat Straw. *Biotechnol. Biofuels* **2009**, *2* (31), 1−14.
(31) Foust, T.; Aden, A.; Dutta, A.; Phillips, S. An economic and environmental Comparison of a biochemical and a thermochemical lignocellulosic ethanol conversion processes. *Cellulose* **2009**, *16*, 547−565.
(32) Dunlop, A. P. Furfural formation and behavior. *Ind. Eng. Chem.* **1948**, *40*, 204−209.
(33) McKibbins, S. W.; Harris, J. F.; Saeman, J. F.; Neill, W. K. Kinetics of the acid catalyzed conversion of glucose to 5-hydroxymethyl-2-furaldehyde and levulinic acid. *Forest Prod. J.* **1962**, *5*, 17−23.
(34) Qian, X. H.; Nimlos, M. R.; Davis, M.; Johnson, D. K.; Himmel, M. E. AbInitio molecular dynamics simulations of beta-D-glucose and beta-D-xylose degradation mechanisms in acidic aqueous solution. *Carbohydr. Res.* **2005**, *340*, 2319−2327.
(35) Palmqvist, E.; Hahn-Hagerdal, B. Fermentation of lignocellulosic hydrolysates. II: inhibitors and mechanisms of inhibition. *Bioresour. Technol.* **2000**, *74*, 25−33.
(36) Cantarella, M.; Cantarella, L.; Gallifuoco, A.; Spera, A.; Alfani, F. Effect of inhibitors released during steam-explosion treatment of poplar wood on subsequent enzymatic hydrolysis and SSF. *Biotechnol. Prog.* **2004**, *20*, 200−206.
(37) Klinke, H. B.; Thomsen, A. B.; Ahring, B. K. Inhibition of ethanol-producing yeast and bacteria by degradation products produced during pre-treatment of biomass. *Appl. Microbiol. Biotechnol.* **2004**, *66*, 10−26.
(38) Baxter, L. L.; Miles, T. R.; Jenkins, B. M.; Milne, T.; Dayton, D.; Bryers, R. W.; Oden, L. L. The Behavior of Inorganic Material in Biomass-Fired Power Boilers: An Overview of the Alkali Deposits Project. In *Developments in Thermo-Chemical Biomass Conversion*; Bridgwater, A. V., Boocock, D. G. B., Eds.; Blackie Academic and Professional: London, 1997; Vol. *1/2*.
(39) Blander, M.; Pelton, A. D. The inorganic chemistry of the combustion of wheat straw. *Biomass Bioenergy* **1997**, *12*, 295−298.
(40) Ankra, K. Studies of Black Silica Produced under Varying Conditions. Ph.D. Thesis, University of California, Berkeley, 1975.
(41) Brunauer, S.; Emmett, P. H.; Teller, E. Adsorption of gases in multimolecular layers. *J. Am. Chem. Soc.* **1938**, *60*, 309−319.
(42) Heiri, O.; Lotter, A. F.; Lemcke, G. Loss on ignition as a method for estimating organic and carbonate content in sediments: Reproducibility and comparability of results. *J. Paleolimnol.* **2001**, *25*, 101−110.
(43) Jones, J. M.; Darvell, L. I.; Bridgeman, T. G.; Pourkashanian, M.; Williams, A. An investigation of the thermal and catalytic behavior of potassium in biomass combustion. *Proc. Combust. Inst.* **2007**, *31*, 1955−1963.
(44) Ponder, G. R.; Richards, G. N. Pyrolysis of Some ^{13}C-labeled Glucans: a Mechanistic Study. *Carbohydr. Res.* **1993**, *244*, 27−47.
(45) Evans, R. J.; Milne, T. A. Molecular Characterization of the Pyrolysis of Biomass: 1. Fundamentals. *Energy Fuels* **1987**, *1*, 123−137.
(46) Shafizadeh, F. Introduction to pyrolysis of biomass. *J. Anal. Appl. Pyrolysis* **1982**, *3*, 283−305.
(47) Olsson, J. G.; Jaglid, U.; Pettersson, J. B. C.; Hald, P. Alkali metal emission during pyrolysis of biomass. *Energy Fuels* **1997**, *11*, 779−784.
(48) Ahmad Alyosef, H.; Ibrahim, S. S.; Welscher, J.; Inayat, A.; Eilert, A.; Denecke, R.; Schwieger, W.; Münster, T.; Kloess, G.; Einicke, W.-D.; Enke, D. Effect of acid treatment on the chemical composition and the structure of Egyptian diatomite. *Int. J. Miner. Process.* **2014**, *132*, 17−25.
(49) Rawle, A. The importance of particle sizing to the coatings industry, Part 1: Particle size measurement. *J. Color Sci. Technol.* **2002**, *5*, 1−12.
(50) IUPAC recommendations for the characterization of porous solid (Technical Report). *Pure Appl. Chem.* **1994**, *66* (8), 1739-1758.10.1351/pac199466081739
(51) Gregg, S. J.; Sing, K. S. W. *Adsorption, Surface Area and Porosity*, 2nd ed.; Academic Press INC: New York, 1991; pp 111−190.

DOI: 10.1021/acssuschemeng.5b00275
ACS Sustainable Chem. Eng. 2015, 3, 2012−2021